Supersonic Rectangular Jet Impingement Noise Experiments

Thomas D. Norum*
NASA Langley Research Center, Hampton, Virginia 23665

The discrete frequency sound produced by jets issuing from a convergent, rectangular nozzle of aspect ratio 4.24 was investigated. Experiments were performed both with the free jet and with the jet impinging on a hard ground surface. Fully expanded Mach numbers to 1.95 were attained. Measurements of both shock cell length and screech wavelength of the free jet show excellent agreement with theory. The impingement tones that dominate the impinging jet spectra show a definite staging behavior that appears to be biased toward the free jet screech frequency once the separation distance exceeds the region of substantial shock cell development. The frequency variation of the impingement tone stages fits the details of a feedback cycle if the disturbance convection velocity is chosen to be 20% higher than that necessary to satisfy the screech feedback loop. Phase locked optical records show a flapping mode of jet oscillation with tones at or near the screech frequency, with superimposed symmetric oscillations when a second dominant tone of unrelated frequency appears in the spectrum.

Nomenclature

a = ambient sound speed
b = breadth (long dimension) of nozzle exit, 2.013 in.
f = frequency of screech tone or impingement tone
h = distance between nozzle exit and ground surface
L = shock cell length
M_j = fully expanded jet Mach number
n = number of periods of sound wave in feedback loop
V_c = average convection velocity
V_j = fully expanded velocity
V_ℓ = loop velocity, $V_c/(1 + V_c/a)$
w = width (short dimension) of nozzle exit, 0.475 in.
x = axial distance
x_2 = distance parallel to nozzle short exit dimension
x_3 = distance parallel to nozzle long exit dimension
α = ratio of convection to fully expanded velocities
λ = wavelength of screech tone

Introduction

THE pressure fluctuations generated by the impingement of a supersonic jet on a solid surface has application to aircraft with thrust vectoring as well as short takeoff and vertical landing capabilities. The noise produced in the impingement process as well as the dynamic pressures in the deflected flow may dictate the fatigue life of the aircraft structure in the vicinity of the exhaust nozzles. Hence, a good understanding of the noise generation mechanisms in this complex flowfield is desired. The most dominant of these mechanisms, that which produces discrete frequency sound, is the subject of this paper.

Of the many investigations into the noise generated by impinging jets, most have dealt with subsonic flow. At subsonic speeds above Mach number 0.7 and nozzle exit to surface distances of a few nozzle diameters, a resonant condition exists and the noise field is dominated by a single frequency. This was studied in detail by Ho and Nosseir.[1] Powell[2] reported on the oscillations produced by round supersonic jets impinging on surfaces of various sizes and presented a good list of references for impingement studies, noting that few details of the noise produced under supersonic conditions have been reported. Exceptions are Krothapalli,[3] who reported on the tones emitted by two-dimensional underexpanded impinging jets, and the works of Ahuja et al.,[4,5] who obtained detailed near-field noise measurements of round impinging jets at Mach numbers of 0.8 and 1.4.

A rectangular jet was chosen over a round jet for the present study, due both to the longer optical path for photographs of the flow and to avoid the multiple modes of screech present in an underexpanded round jet. The objectives of this work are to detail the discrete noise processes for both the free jet and the jet impinging on a surface over the complete range of nozzle-to-surface distances and over a wide range of nozzle pressure ratios.

Description of Experiment

The experiments were performed in the Quiet Flow Facility of the NASA Langley Noise Reduction Laboratory. This anechoic chamber has dimensions 20 × 24 × 30 ft and is lined with wedges to permit acoustic measurements down to 70 Hz. Details of the facility can be found in Ref. 6.

The rectangular nozzle was fed from a high-pressure air supply system via a 3-in. supply pipe. A transition piece, following the supply pipe, changed the 3-in. internal diameter to a 2 × 2-in. square over an axial distance of 8 in. This connected to the nozzle itself, which consisted of a constant square cross section for an axial distance of 6 in., followed by an additional 6 in. in which a pair of opposite walls converged at an angle of 7 deg. This resulted in a rectangular exit cross section with measured breadth b = 2.013 in. and width w = 0.475 in., giving an aspect ratio of 4.24. The nozzle was originally designed for a thrust reverser application and, hence, had a large wall thickness near its exit (see Fig. 1). Heat was supplied to the air supply to maintain its stagnation temperature equal to the chamber ambient temperature.

The nozzle was first operated without the presence of a ground surface in three modes: first, using a linear array of microphones to survey the acoustic near and far fields with acoustic wedges covering the floor; second, using total and static pressure probes to investigate the jet plume via a digitally controlled traversing mechanism; and, third, using optical equipment to obtain phase locked shadowgraph and schlieren records. This was followed by operating the nozzle over the same range of nozzle pressure ratios in the presence of a simulated ground surface. This surface consisted of a 42-in.-diam aluminum disk movable in the jet direction by a digital

Received Aug. 14, 1989; revision received Nov. 16, 1989; accepted for publication June 6, 1990.

*Research Engineer, Acoustics Division, Mail Stop 461. Member AIAA.

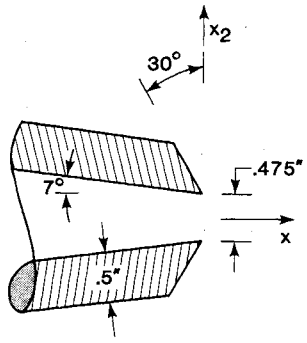

Fig. 1 Lateral cross section of nozzle near its exit.

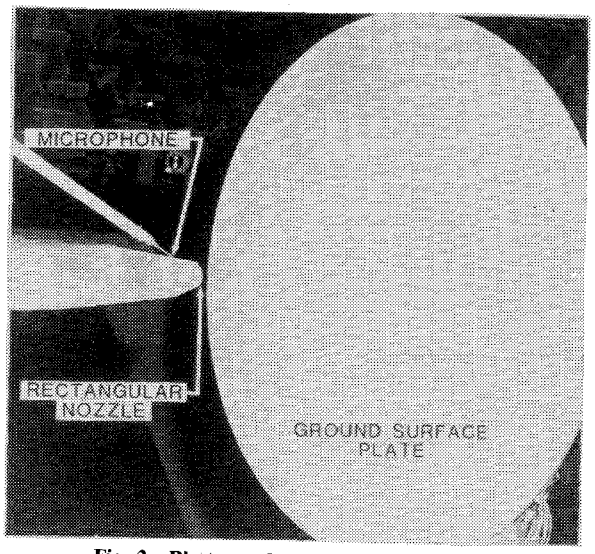

Fig. 2 Photograph of experimental setup.

traverse. Fluctuating pressures were obtained by far-field microphones and by dynamic pressure transducers located on the nozzle external wall and ground surface.

An additional microphone (shown in Fig. 2) was present during all modes of testing. This one-eighth inch condenser microphone was located in the plane containing the jet centerline and parallel to the small nozzle dimension. It was positioned 1.4 in. upstream of the jet exit and 0.5 in. from the nozzle surface. All acoustic data presented in this article were obtained from this microphone.

Free Jet

The nozzle was operated up to a nozzle pressure ratio of 7.3, which corresponds to a fully expanded Mach number of 1.95. The spreading characteristics of the jet at this Mach number were determined by traversing a total pressure probe in the plane perpendicular to the jet direction at sufficient downstream distances for the shock structure to have substantially decayed. The jet boundary, as defined by the position where the impact pressure falls to 10% above the ambient pressure, is shown in Fig. 3. This boundary was determined for traverses parallel to both the short and long dimensions of the nozzle exit. It is clear that a "crossover" in the dimensions of the jet cross section occurs close to the nozzle exit, showing that the jet width spreads much more rapidly than its breadth.

Static pressure surveys along the jet centerline were obtained to detail the shock structure within the supersonic jet. These were obtained with the probe designed by Pinckney[7] specifically for supersonic flow. Results are shown in Fig. 4, in which the vertical scale is given for only every third profile. The amplitudes of the static pressure peaks decay rapidly for fully expanded Mach numbers up to about 1.7. A comparison with unpublished data for a parallel exit flow rectangular nozzle shows identical shock cell spacing and initial shock

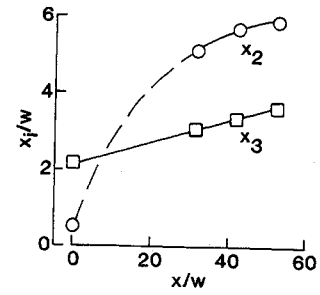

Fig. 3 Free jet boundaries in both lateral directions at $M_j = 1.95$.

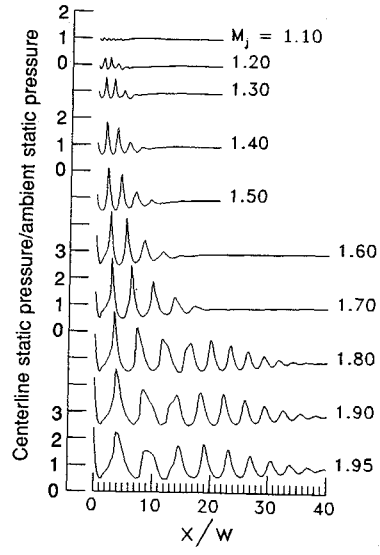

Fig. 4 Centerline static pressure distributions in free jet.

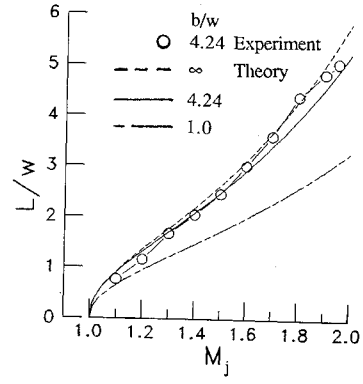

Fig. 5 Shock cell spacing in free jet.

strength, but that the decay of the pressure peaks is more rapid for the 7 deg convergent nozzle of the present experiment, resulting in fewer shock cells. Figure 4 shows that the static pressure decay at Mach numbers 1.8 and above is more gradual than that at the lower speeds, resulting in a large increase in the number of indicated shock cells.

Since at least four pressure peaks can be identified for each pressure profile of Fig. 4, the characteristic shock cell length L is chosen to be equal to the average of the second through fourth shock cell spacings, i.e., one-third the distance between the first and fourth pressure peaks. This measured average shock cell length is given in Fig. 5, along with the shock cell spacing as predicted from the theory of Tam.[8] Figure 5 shows that Tam's prediction for a rectangular nozzle of aspect ratio 4.24 is much closer to that of a two-dimensional nozzle than that of a square nozzle, and that the measured results agree quite well with the theory.

Sound pressure level spectra from the microphone positioned just upstream of the nozzle exit are shown in Fig. 6. For

most supersonic jet operating conditions, the spectra are dominated by a single screech mode consisting of a fundamental tone and its harmonics. The peak spectrum level, corresponding to the fundamental screech tone, is plotted in Fig. 7. It is seen that screech is very strong for Mach numbers between 1.15 and 1.75. Beyond the latter speed, the screech process becomes less dominant, resulting in less violent oscillations of the jet and the stabilization of the shock structure that was seen in the pressure profiles of Fig. 4.

The prediction of the frequency of screech tones, edge tones, and impingement tones has been well-established in the literature based on simple feedback models. The feedback loop consists of disturbances traveling downstream in the jet at an average convection velocity V_c, and sound waves traveling outside the jet at the ambient speed of sound, a. The half-length x of the feedback loop is the distance h between the nozzle exit and the solid surface for edge tones or impingement tones, and the distance L between shock cell ends (i.e., the shock cell length) for screech tones. Specifying the loop traverse time to be an integral number of periods of the sound wave (which is equivalent to assuming that an integral number of waves exist in the feedback loop, as specified by Ho and Nosseir[1]) determines the loop Strouhal number fx/V_ℓ to be an integer n, where V_ℓ is the loop velocity, $V_c/(1 + V_c/a)$.

The value of the fundamental screech tone frequency predicted by Tam[8] is given by $fL/V_\ell = 1$. A comparison between measurement and prediction can be made once the average convection velocity is determined. It is generally assumed that the convection velocity is a fraction of the fully expanded velocity, i.e., $V_c = \alpha V_j$, although some measurements indicate that the convection velocity is also frequency dependent. Various studies of both broadband and discrete frequency jet noise generation from both subsonic and supersonic jets suggest a value of α between 0.5 and 0.7. A comparison of the wavelength computed from the fundamental screech tone frequency with Tam's prediction was made with α varying over this range. A best fit was obtained for $\alpha = 0.52$, and the results shown in Fig. 8. As with the shock cell spacing of Fig. 5, excellent agreement with the prediction is obtained. Combining the results of Figs. 5 and 8 yields the loop Strouhal number data shown in Fig. 9. The fact that the loop Strouhal number is essentially unity (i.e., $n = 1$) over the entire Mach number range indicates that the presumptions of the feedback process are fulfilled for screech if the convection velocity is taken to be 52% of the fully expanded velocity.

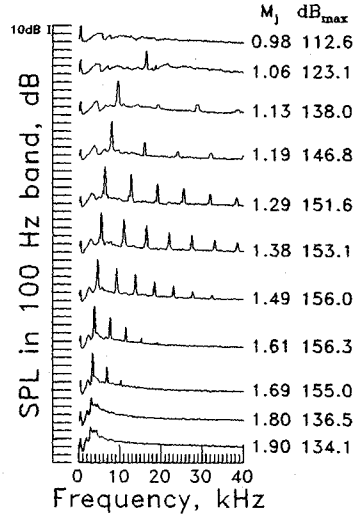

Fig. 6 Free jet spectra from microphone upstream of nozzle exit.

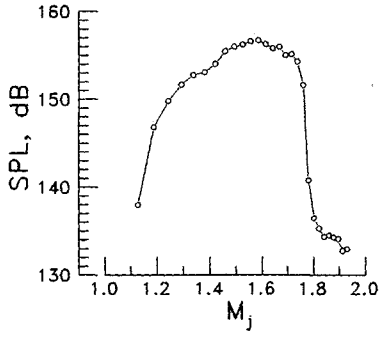

Fig. 7 Amplitude variation with fully expanded Mach number of free jet fundamental screech tone.

Jet Impingement

The microphone signal obtained with the free jet was basically unchanged when the ground surface was installed at a large distance from the jet exit. As the surface approached the jet, the screech tone amplitudes began to vary and other

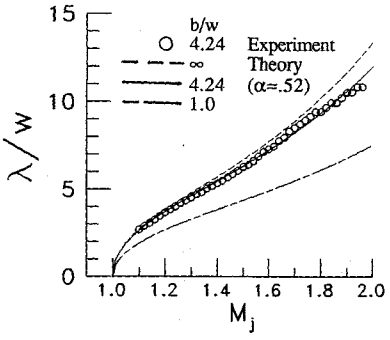

Fig. 8 Wavelength variation with fully expanded Mach number of free jet fundamental screech tone.

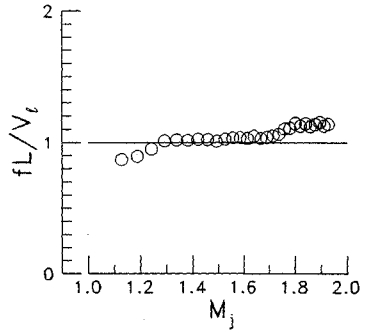

Fig. 9 Loop Strouhal number variation with fully expanded Mach number of free jet fundamental screech tone, $\alpha = 0.52$.

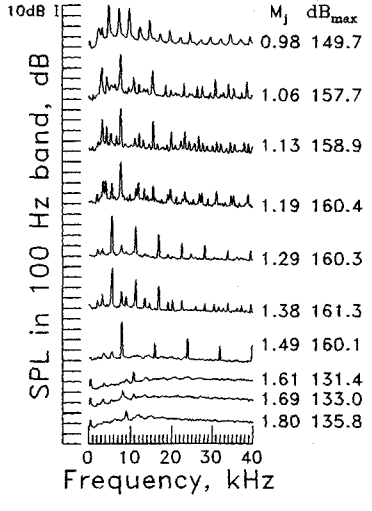

Fig. 10 Impinging jet spectra from microphone upstream of nozzle exit for $h/w = 4.2$.

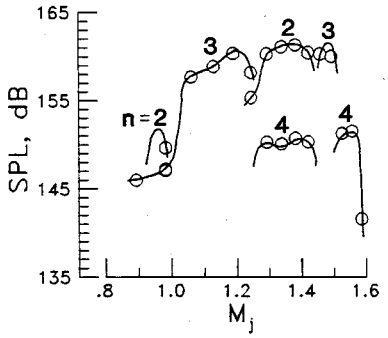

Fig. 11 Amplitude variation with fully expanded Mach number of strongest impingement tones for $h/w = 4.2$.

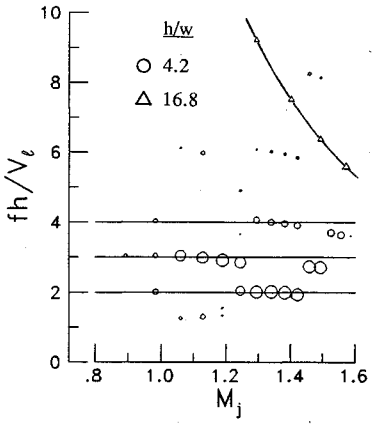

Fig. 12 Loop Strouhal number variation with fully expanded Mach number of strongest tones from impinging jet, $\alpha = 0.63$.

tones began to appear in the spectra. At small nozzle to ground distances, these impingement tones dominate the spectra and the screech tones disappear. Samples of spectra obtained for the latter case at a separation distance of 4.2 nozzle widths are given in Fig. 10. At some Mach numbers the spectra are similar to the free jet spectra, being dominated by a given mode of oscillation, consisting of a fundamental tone and its harmonics. The multitude of tones at other Mach numbers, however, indicate the existence of at least a second mode, as the various tones appear to consist of two independent frequencies together with multiple sums and differences of these frequencies.

Frequency analysis of the dominant tones generated in the impingement process consistently led to the conclusion that the presumption of an integral number of waves in the feedback loop was best met if α was chosen to be 0.63, in contrast to the value of 0.52 that was needed for the screech process. This is very close to the value of $\alpha = 0.62$ obtained by Ho and Nosseir[1] from near-field microphone correlations during their subsonic impinging jet experiments. Krothapalli[3] inferred $\alpha = 0.52$ from schlieren photographs of a Mach number 1.7 impinging jet at a separation distance of 17.6 nozzle widths. This is also in agreement with the present results, since the jet is likely dominated by the screech process at this condition. Hence, it appears that the effective convection velocity is about 20% higher in the impingement process than in the screech process.

The strengths of the largest amplitude tones at $h/w = 4.2$ are given in Fig. 11. These tones are separated into stages, with stage number n equal to the number of waves in the feedback loop, as determined from the frequency analysis. Although the tone amplitudes are certainly dependent on the separation distance, this figure is representative of impingement tones and can be used to compare to the free jet screech tone amplitudes given in Fig. 7. At high subsonic Mach numbers, where free jet screech tones cannot exist, strong impingement tones

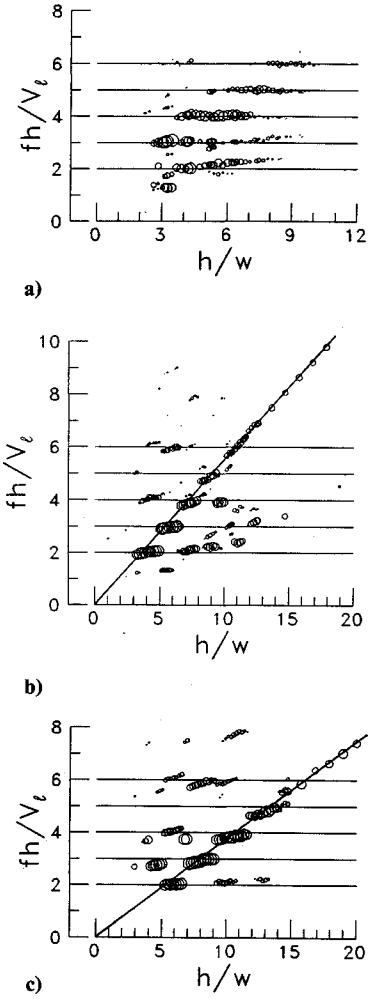

Fig. 13 Loop Strouhal number variation with separation distance of strongest tones for impinging jet, $\alpha = 0.63$: a) $m_j = 0.98$; b) $m_j = 1.29$; c) $m_j = 1.49$.

appear in the spectra. At supersonic conditions, they increase in amplitude and reach a maximum about 5 dB higher than the strongest free jet screech tones. The impingement tones are greatly reduced by a Mach number of 1.6, a condition at which screech tones still dominate the free jet spectra.

The frequency variation of the impingement tones at this separation distance of $h/w = 4.2$ is given in Fig. 12. Shown is the loop Strouhal number vs fully expanded Mach number, where the convection velocity was computed with $\alpha = 0.63$. The height of the symbols is proportional to the tone sound pressure level minus 140 dB, so that tone dominance is illustrated by the symbol size. It is seen that the dominant tone corresponds to 2, 3, or 4 waves in the feedback loop, depending on the Mach number. The triangular symbols given in Fig. 12 correspond to the loop Strouhal number of the dominant tone at a separation distance $h/w = 16.8$. Its large variation with M_j indicates screech rather than impingement is the dominant noise generation mechanism at this larger separation distance.

A better depiction of the delineation between screech and impingement processes is obtained by holding the nozzle pressure ratio constant and increasing the nozzle-to-ground separation distance. The loop Strouhal numbers thus obtained at fully expanded Mach numbers of 0.98, 1.29, and 1.49 are given in Figs. 13a–13c. As in Fig. 12, the symbol size in these figures is proportional to the tone sound pressure level above 140 dB (except for $M_j = 0.98$, in which 130 dB was used as the minimum).

Definite staging behavior typical of edge tones and impingement tones is seen in the high subsonic case of Fig. 13a. The dominant stage number n generally increases from 3 to 6 as

h/w is increased. Since a shock structure does not exist to support the screech process, the measured spectra become toneless at large separation distances. Similar staging behavior of the impingement tones exists in the supersonic cases of Figs. 13b and 13c. Stage numbers 2–5 can be identified in both figures, and strong impingement tones can be seen up to a separation distance of about 10 or 15 nozzle widths. At larger h/w, the spectra are dominated by screech, the fundamental frequency of which is given by the sloping straight line.

At small values of h/w at $M_j = 1.49$ in Fig. 13c, the dominant impingement tone varies randomly between stages 2, 3, and 4. The jump to stage 3 occurring at $h/w = 7$ and the jumps to successively higher stages at larger h/w are such to keep the dominant impingement tone frequency close to the screech frequency. Similar behavior is evident at $M_j = 1.29$ in Fig. 13b, where the jump to stage 3 occurs at $h/w = 5$. It can be seen from Fig. 4 that the location for this jump to stage 3 corresponds in both cases to the location of the end of the last strong (third) shock cell in the free jet. Since the flow is supersonic, the presence of the ground surface should not have a major influence on upstream shock cell development, and hence the observation that the preferred frequency of the impingement process at larger h/w is the same as that of the screech process may not be unexpected.

The amplitude of the loudest tone for the conditions of Figs. 13a–13c are shown in Figs. 14a–14c. It can be seen that the impingement tones are very strong in all three cases beyond a separation distance of about three nozzle widths. As noted in Fig. 13, the tones die out for the subsonic case at separation distances much beyond $10w$, whereas the maximum tone levels for the supersonic cases at large separation distances approach their respective free jet screech tone levels. There are small perturbations in the amplitude distribution for large h/W at $M_j = 1.49$ in Fig. 14c (perturbations that become larger at higher Mach numbers are not shown here). The physical distance between successive minima in the amplitude distribution was computed to be equal to a half wavelength of the screech tone. This indicates that these perturbations are caused by interference due to sound waves reflected from the ground plate in the same manner as occurs when a reflector is located upstream of the nozzle exit.[9]

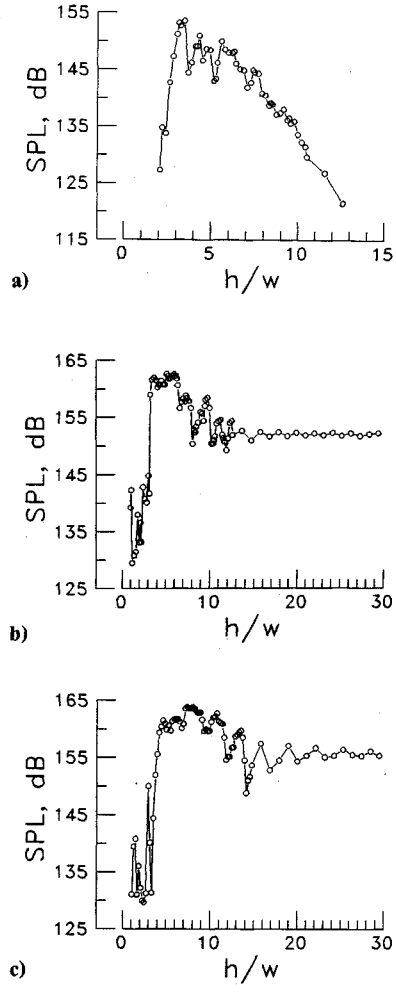

Fig. 14 Amplitude variation with separation distance of strongest tones for impinging jet: a) $m_j = 0.98$; b) $m_j = 1.29$; c) $m_j = 1.49$.

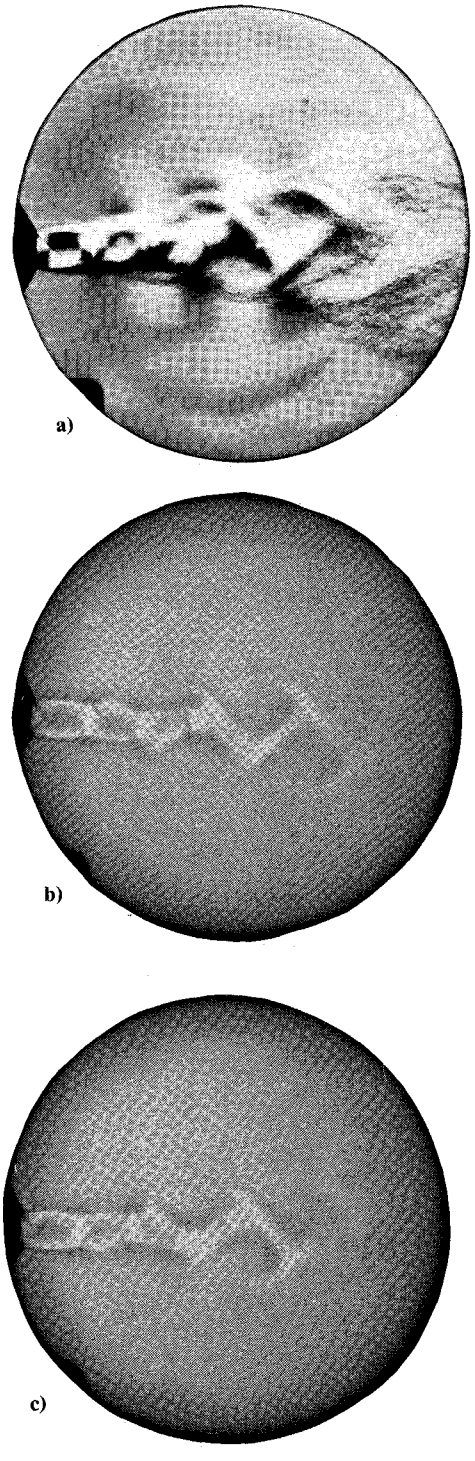

Fig. 15 Optical records at screech frequency of impinging jet ($M_j = 1.29$, $h/w = 26$, $f = 6.4$ kHz): a) schlieren; b) shadowgraph at 0 deg; c) shadowgraph at 180 deg.

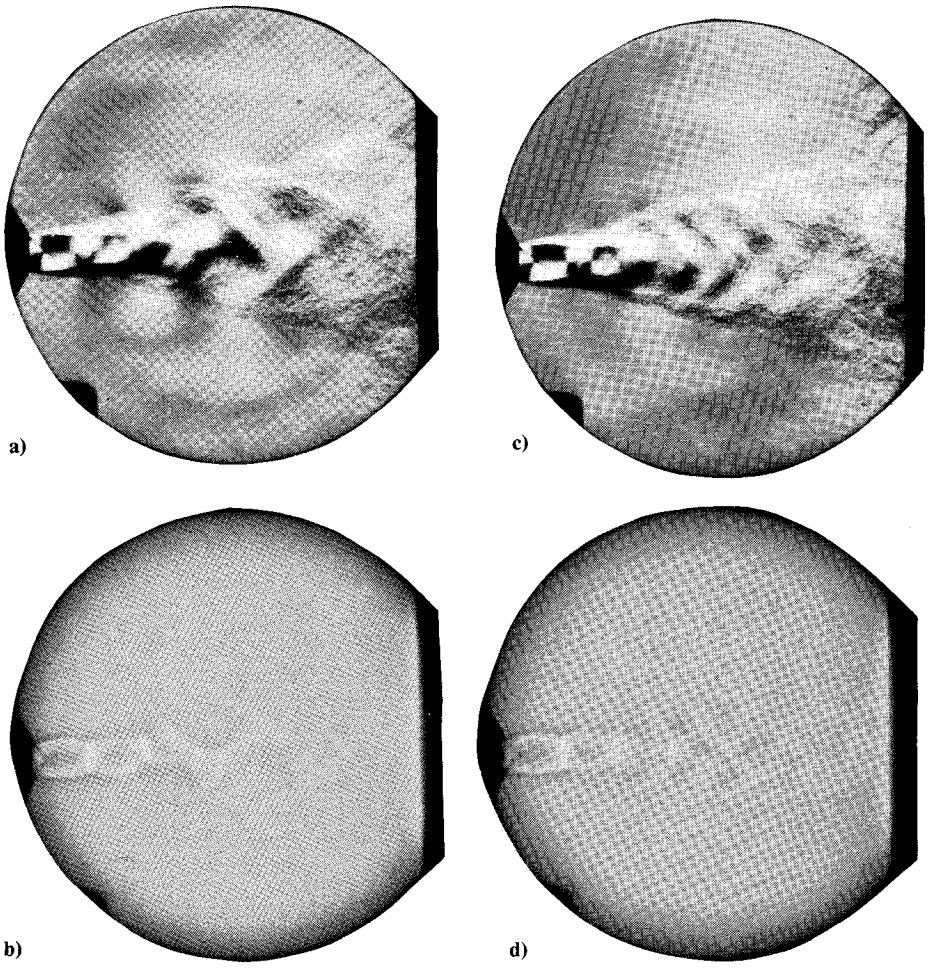

Fig. 16 Optical records at dominant frequencies of impinging jet (M_j = 1.29, h/w = 11): a) schlieren, f = 6.4 kHz; b) shadowgraph, f = 6.4 kHz; c) schlieren, f = 2.6 kHz; d) shadowgraph, f = 2.6 kHz.

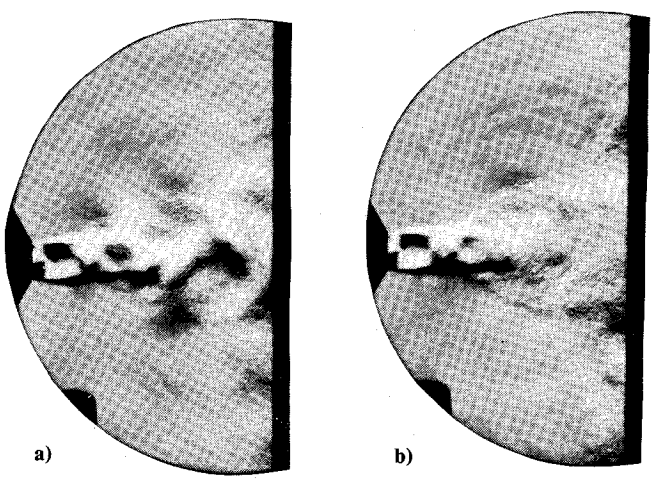

Fig. 17 Schlieren photographs at dominant frequencies of impinging jet (M_j = 1.29, h/w = 7.3): a) f = 6.4 kHz; b) f = 3.5 kHz.

Flow Visualization

The manner in which the jet oscillates can be seen through flow visualization. Optical records were obtained using a stroboscopic point source (0.1 mm × 1 mm) capable of operating at 10,000 flashes per second, with a pulse width of less than 1 μs. The light was collimated with two 6-in. mirrors and the optical image recorded on either videotape or 70 mm photographic film. Presented in this section are photographs taken perpendicular to the narrow edge of the nozzle. Included are optical records obtained by both the shadowgraph method and the schlieren method, with the knife edge parallel to the flow direction. The light source was activated by the microphone signal filtered around the frequency of a strong tone, so that each photograph resulted from a controlled number of light pulses at a given phase of this tone.

Optical records obtained by activating the strobe at the screech fundamental frequency with the jet operating at a fully expanded Mach number of 1.29 and h/w = 26 are shown in Figs. 15a–15c. At this large separation distance, both the photographs and the measured acoustic signal were essentially identical to those obtained for the free jet. The phase-averaged schlieren in Fig. 15a shows acoustic waves being emitted by the jet at positions beginning at the end of the second shock cell and extending at least beyond the location of the fourth cell. The shadowgraphs in Figs. 15b and 15c were obtained with a 180 deg difference in the phase of the activating microphone signal. The mirror images of these two shadowgraphs show that the jet is definitely oscillating in the asymmetric flapping mode. The large amplitude of the oscillations explains the rapid spreading of the jet in the direction parallel to the small dimension of the nozzle. This also explains why there are only a few shock cells apparent in the centerline static pressure traverses.

Moving the ground surface to h/w = 11 at the same Mach number yields the photographs in Figs. 16a–16d. The acoustic spectrum at this location shows two dominant tones of equal amplitude at unrelated frequencies. Figures 16a and 16b correspond to strobe activation at the screech frequency and show oscillations very similar to those seen in Fig. 15. Strobe activation by the other lower frequency tone results in the photographs of Figs. 16c and 16c. Here the oscillation appears to be symmetric, indicating a pulsing motion rather than the flap-

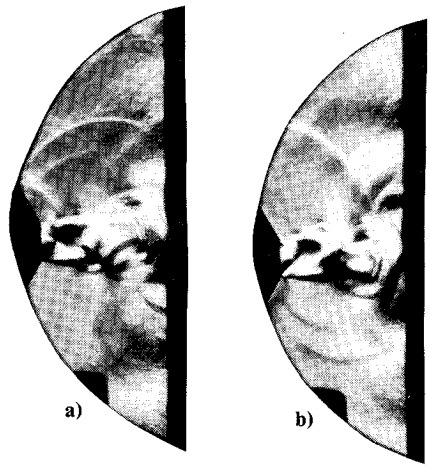

Fig. 18 Schlieren photographs at dominant impingement tone frequency (M_j = 1.29, h/w = 4.1, f = 5.9 kHz): a) 0 deg; b) 180 deg.

Fig. 19 Schlieren photograph at dominant impingement tone frequency (M_j = 0.98, h/w = 4.3, f = 4.9 kHz).

ping motion that occurs at the screech frequency. This axial pulsing is very evident in the video recording.

Further visual evidence that the total jet oscillation can be composed of multiple modes is seen in Figs. 17a and 17b. Here h/w has been reduced to 7.3, and again the acoustic spectrum is dominated by two tones. These tones were shown in the frequency analysis of Fig. 13b to correspond to n = 4 and n = 2, respectively, although the spectral data show that the higher frequency is definitely not exactly twice the other and, hence, they are not harmonics. Strobe activation by the impingement tone whose frequency is close to that of the free jet screech tone shows the asymmetric oscillation given in Fig. 17a. Strobing at the lower frequency results in Fig. 17b, which indicates a symmetric flow similar to that obtained in Fig. 16c. It is interesting to note that both Figs. 17a and 17b show acoustic waves that appear to be emanating from a region of the jet located halfway between the nozzle exit and the impingement surface, as well as from the region of jet impingement.

Reducing the separation distance even further, to h/w = 4.1, results in an acoustic spectrum dominated by a single impingement tone and its harmonics. This tone corresponds to n = 2 and has a frequency close to the free jet screech tone. Phase locked schlierens taken at this condition are shown in Figs. 18a and 18b. The two photographs differ due to a 180 deg phase difference in their respective strobe activation signals. Strong acoustic waves are again seen to be emanating both from the jet itself and from the impingement region. Also evident are waves that have been reflected from the massive nozzle walls.

A schlieren photograph of the jet operating at a fully expanded Mach number of 0.98 with h/w = 4.3 is shown in Fig. 19. The jet is seen to be oscillating in a flapping mode at the dominant frequency of the impingement process. From other photographs not reproduced here, oscillations of this transonic jet at other impingement tone frequencies appear to occur in a symmetric mode, although the symmetric oscillations are not as obvious as the asymmetric ones shown in Fig. 19.

Conclusions

A convergent rectangular nozzle of aspect ratio 4.24 was operated at fully expanded Mach numbers up to 1.95, both in the free jet mode and impinging on a solid ground surface. Photographs of the free jet, phase locked at the screech frequency by a microphone signal, show very large amplitude jet oscillations parallel to the short dimension of the nozzle. These oscillations contribute to the crossover of jet dimensions evident in mean total pressure profiles. Centerline static pressure traverses provide evidence of only about four shock cells up to a nozzle pressure ratio above which the screech amplitudes fall dramatically. At higher pressure ratios, the reduction of screech amplitude apparently coincides with smaller lateral oscillation of the jet, which allows for the development of the more extensive shock cell system measured at these conditions. The measured shock cell spacing agrees well with the theory of Tam over the entire range of supersonic operating conditions. The feedback model of screech also predicts the frequency of the oscillations if the average convection velocity is chosen to be 52% of the fully expanded jet velocity.

The noise generated by impinging the jet on a solid ground surface consists of multiple tones for many operating conditions. Phase locked photographs show evidence of axial oscillations of the jet in addition to the lateral oscillations that are also present in the free jet. The maximum amplitudes of the impingement tones occur at separation distances between 3 and 10 nozzle exit widths, and occur over a lower Mach number range than do the maximum amplitudes of the screech tones. The frequencies of the impingement tones show a definite staging behavior and can be predicted well by a feedback model with an average convection velocity equal to 63% of the fully expanded velocity, or 20% higher than that needed to satisfy the screech model. Once the separation distance between the nozzle exit and ground plane is beyond the region of the first few shock cells of the free jet, the jumps in frequency to the next stage occur so as to keep the dominant impingement tone frequency close to that of the free jet screech tone.

References

[1]Ho, C. H., and Nosseir, N. G., "Dynamics of an Impinging Jet. Part 1. The Feedback Phenomenon," *Journal of Fluid Mechanics,* Vol. 105, April 1981, pp. 119–142.

[2]Powell, A., "The Sound-Producing Oscillations of Round Underexpanded Jets Impinging on Normal Plates," *Journal of Acoustical Society of America,* Vol. 83, No. 2, 1988, pp. 515–533.

[3]Krothapalli, A., "Discrete Tones Generated by an Impinging Underexpanded Rectangular Jet," *AIAA Journal,* Vol. 23, No. 12, 1985, pp. 1910–1915.

[4]Ahuja, K. K., and Spencer, D. A., "Aeroacoustics of Advanced STOVL Aircraft Plumes," *Proceedings of International Powered Lift Conference,* Santa Clara, CA, Dec. 1987, Society of Automotive Engineers, Inc., Warrendale, PA, 1988, pp. 531–541.

[5]Ahuja, K. K., Tam, C. K. W., Salikuddin, M., Burrin, R. H., and Roads, R., "Aeroacoustic Environment of Single and Twin Impinging Model Plumes in Relation to Advanced STOVL Aircraft," NASA CR-4291, 1990.

[6]Hubbard, H. H., and Manning, J. C., "Aeroacoustic Research Facilities at NASA Langley Research Center—Description and Operational Characteristics," NASA TM-84585, 1983.

[7]Pinckney, S. Z., "A Short Static-Pressure Probe Design for Supersonic Flow," NASA TN D-7978, 1975.

[8]Tam, C. K. W., "The Shock-Cell Structures and Screech Tone Frequencies of Rectangular and Non-Axisymmetric Supersonic Jets," *Journal of Sound and Vibration,* Vol. 121, No. 1, 1988, pp. 135–147.

[9]Norum, T. D., "Control of Jet Shock Associated Noise by a Reflector," AIAA Paper 84-2279, Oct. 1984.